Progress in the Visualization of Filamentary Gas Discharges. Part 2: Visualization of DC Positive Corona Discharges

Jerzy Mizeraczyk[1,*], Seiji Kanazawa[2], and Toshikazu Ohkubo[2]

[1]Centre for Plasma and Laser Engineering, Institute of Fluid Flow Machinery, Polish Academy of Sciences, 80-231 Gdańsk, Poland
[2]Department for Electrical and Electronic Engineering, Faculty of Engineering, Oita University, 700 Dannoharu, Oita, 870-1192, Japan

***Abstract*:** Recently the filamentary gas discharges at atmospheric pressure, such as dielectric-barrier and corona discharges regained their importance due to numerous new applications. These new applications impose a demand of better understanding of the fundamentals of the filamentary discharges. As a consequence, during the last ten years an essential progress in the diagnostics of the filamentary discharges has been made. The recent progress in the investigations of the dielectric-barrier discharges by cross-correlation spectroscopy was described in Part 1 of this paper. Part 2 is a survey of the recent progress in the visualization of DC positive corona discharges.

Introduction

Recently the filamentary discharges, such as dielectric-barrier discharges (DBDs) and corona discharges once more became of high interest because of their new applications in industry. The recent applications of DBDs are described briefly in Part 1. During the last 20 years the corona discharges became of interest because of their potential to be utilized in new technologies for the plasmo-chemical treatment of gases and liquids (for example for the removal of SO_2 and NO_x from flue gases, destruction of other hazardous gaseous pollutants, and conversion of hydrocarbons) (*1-9*). However, the progress in the implementation of corona discharges for environmental purposes is slow. This is mainly caused by the poor understanding of corona discharges in spite of almost 100-year history of the investigation of the filamentary discharges, including the corona discharges [for example, see (*10-14*)]. The poor understanding of corona discharges is due to the complexity of physical and chemical phenomena, which occur in the spatially and temporally complex plasma of corona discharges. These phenomena could not be studied with the required spatial and temporal resolution due to the lack of the appropriate equipment. Recent progress in the development of Charge Coupled Device (CCD) cameras, imaging spectrographs and fast digital image processing has made the investigation of the filamentary discharges possible with higher sensitivity and spatial and temporal resolution than ever. In this paper an overview of the recent progress in the visualization of DC positive corona discharges with advanced CCD cameras is given.

Keywords: corona discharge, non-equilibrium plasma, plasma diagnostics, discharge visualization, plasma chemistry

*E-mail: jmiz@imp.gda.pl

Basic Properties of Corona Discharges

Corona discharges belong to a group of transient non-thermal plasma discharges. The existence of the transient discharge depends on the space charge movement in the electric field. If this movement stops for some reason then the space charge diffuses and recombines, the current goes to zero and eventually the discharge extinguishes. Therefore it is called a transient discharge.

Various aspects of the transient discharges, including coronas were described in standard books on gas discharges and plasma physics [e.g. (*10-14*)]. The present view on the physics of the corona discharges is given in [(*7*), pages 5-21]. Here only the basic properties of the corona discharges, relevant to the main part of this paper, i.e. to the presentation of the state-of-the art of corona discharge visualization, are briefly outlined.

The corona discharge designation refers to the polarity (positive or negative) of the voltage applied to the highly stressed electrode (also called the discharge electrode) in the electrode arrangement, and to the type of the applied voltage (DC, AC or pulsed). Also the corona discharges are distinguished referring to their length, which can be from micrometers to tens of meters. In this paper we deal with DC or pulsed corona discharges of positive or negative polarity in the electrode arrangement of size of several centimeters, which is of importance from the application point of view.

Several electrode arrangements are used to generate corona discharges. They are point-to-plane, nozzle-to-plane, sphere-to-plane, wire-to-cylinder, wire-to-plane, sharp edge-to-plane, etc. In the DC corona discharges the applied voltage is up to several tens of kV, and the current per corona discharge pulse is up to several tens of mA. In the case of pulsed corona discharges, the amplitude of applied voltage is several tens of kV, the amplitude of the discharge pulse is several A. In both cases the discharge pulse duration is in the range of 20-500 ns. The values given above are approximate; in a particular case they may differ significantly from those given above. However, generally the current of the pulsed corona discharge is much higher that the DC case.

The corona discharges can have the form of avalanches, bursts, burst pulses, glows, streamers, and secondary streamers [(*12*), pages 319-383]. The type of the corona discharge, which develops in the gap between the electrodes depends on the electrode geometry, applied voltage and working gas. Here we deal with streamer corona discharges.

A streamer is a well developed corona discharge, which consists of the space charge region formed by positive ions (in the number of 10^8-10^9), called the streamer head, propagating through the working gas towards the cathode, and of the quasi-neutral channel (called the streamer channel), which is formed on the track passed by the streamer head. The streamer head, difficult to be observed, is believed to be a disk of a diameter and thickness of 200 μm and 20 μm, respectively (*15-17*). The streamer head velocity is 10^5-10^6 m/s (*17, 18*).

Several conditions have to be fulfilled to develop a corona into a streamer. To incept a streamer the applied field strength has to be higher than the so-called inception (or critical) field strength, and a certain path on the way towards the anode, called the inception (or critical) distance, has to be available to develop the streamer. The inception field strength in air is about 30 kV cm^{-1} (*12*) and the inception distance is a fraction of a millimeter. Even if both of these conditions are met, the streamer may not start. This stochastic nature of the corona streamer is described by the inception probability. Even if the inception probability is one, the development of an corona avalanche into a streamer needs a time, called the inception time-lag, which is relatively long and has a stochastic uncertainty, called the inception time-lag jitter. The typical time-lag ranges from 0 to 400 ns, depending on the discharge conditions and power suppliers (*17*), see also 5.1.

Another important parameter of the streamer is the maximum field strength. The highest field strength, which can be built around the streamer head by the space charge is called the maximum field strength. Its value is limited by electrostatic repulsion of the positive ion charges in the streamer head, which hinders unlimited increase of the space charge in the streamer head. According to (*17*), the value of the maximum field strength in air can be estimated to be 520 ± 60 Td, which is equivalent to about 170 kV cm^{-1}. This corresponds to the average electron energy of the order of 5-10 eV, which was confirmed also experimentally (*19, 20*).

Once developed the streamer can propagate in an electric field, which strength is much lower than that necessary for its inception. The lowest applied field strength that permits the streamer propagation is called the stability field strength. It was shown theoretically that the electric field strength inside the streamer channel is equal to the stability field [(*7*), pages 21-48, (*15*)]. The stability field strength in air is 5 kV/cm (*21*).

Another inherent property of the corona streamer is its branching. A sufficiently large streamer head may split in parts, propagating further as several almost independent streamers. The branching process may repeat several times on the pathway of the streamer corona discharge to the cathode. The branching depends on the electrode configuration, the gas composition and the power supplier in the case of the pulsed corona (*17*).

A Brief Overview of the Diagnostics of Corona Discharges

Comprehensive experimental investigations of corona discharges were carried out during the last century. They concerned such aspects of the corona discharge as current-voltage characteristics, neutral and charged particle interactions, dynamics of the neutral and charged particles, and branching and propagation of the streamers. Various diagnostics methods were used for these investigations. The reader is referred to the standard books (*10-14*). In this section only the optical methods that were used for the corona discharge visualization are briefly surveyed.

Besides the useful but qualitative way of observing the corona discharge with eyes, photography was very early employed as a method of imaging these discharges. Very interesting images of corona discharges, known as Lichtenberg figures can be found in (*10, 11*). The early imaging of corona discharges by photography were imprecise, due to long exposure time, to be useful in the studies of corona discharges

that are inherently spatially and temporally transient. At that time more details on the development of the electron avalanche into the corona discharge delivered a measurement in which a cloud chamber was used (*22*). Using the cloud chamber made the imaging of the avalanche shape possible.

The methods to record the discharge images with nanosecond time resolution and relatively good spatial resolution are streak and Schlieren photography. The early investigations of the corona discharges using streak photography are presented in (*23, 24*). Recent results on the visualization of the distribution of streamers in the pulsed corona using Schlieren photography are shown in (*20*).

The essential progress in the time-resolved observation of the corona streamer properties was made when a photo-multiplier was employed as a light detector. In combination with a multi-channel analyzer it offered sub-nanosecond resolution, which was sufficient to determine streamer velocity and observe streamer propagation (*25*).

A new possibility in the high spatially and temporally resolved visualization of the corona discharges appeared when Charge Couple Device (CCD) cameras were introduced. The method of the corona discharge visualization using CCD cameras is described in the following chapters.

The advanced CCD cameras also contributed to the development of cross-correlation spectroscopy (CCS), which became a powerful tool to analyze the spatially and temporally resolved structure of the filamentary discharges (see Part 1 of this paper).

Recent Progress in the Visualization of Corona Discharges

Recent technological progress in the development of intensified Charge Coupled Device (ICCD) cameras, imaging spectrographs and fast digital image processing has made visualization of complex gas discharges possible with higher sensitivity and space and time resolution than ever. In particular, it concerns the visualization of the transient filamentary discharges, like DBDs and corona discharges.

The modern ICCD cameras enable recording two-dimensional images of the transient discharges with high spatial and time resolution. The high spatial resolution is obtained owing to the high sensitive small pixel elements of the CCD. The nowadays ICCD cameras have several hundred x several hundred (horizontal x vertical) pixels with a pixel area of about 20 μm x 20 μm. Therefore the spatial resolution of the image is of that order [the spatial resolution of the photographed object (e.g., of a discharge) depends on the magnification of the optics, which projects the object on the CCD element]. The high temporal resolution is a result of the image intensifier placed in the front of the CCD element, which operates as a fast shutter, yielding an (exposure) time of the order of 1 nanosecond in more sophisticated ICCD cameras. Another advantage of the ICCD cameras is linearity of the dependence: output signal-input signal in a high dynamic range (more than 12 bits). This is very important in cases when the light emitted by the discharge changes considerably in time and space, as in the transient DBDs and corona discharges.

For the temporally resolved imaging of corona discharges the synchronisation of the discharge pulse and the opening of the ICCD camera (gate start and exposure time) is a crucial point. The synchronization techniques have to be somewhat different for the DC corona discharges and pulsed corona discharges because of their different features. The DC corona discharge consists of more of less regular self-repetitive current pulses with a pulse duration up to several hundred nanoseconds and repetition frequency in the range of 1 to 100 kHz. When the DC voltage is high enough, the inception probability of each DC corona current pulse is one. However, the inception time-lag of the DC corona current pulse has a jitter. The pulsed corona can consists of current pulses, however each of them is triggered by an external pulsed power supply. When the triggering voltage pulse is high enough, the inception probability of the pulsed corona is one, but still the jittering of the inception time of the corona pulse exists. The repetition rate of the externally triggered corona pulses is controlled by the power supply. It reaches up to 1000 Hz. The pulse duration depends on the power supply and varies from several tens of nanoseconds to several hundred nanoseconds.

In order to perform a temporally resolved imaging of the transient discharge, a reference time must be assigned to the characteristic event related to the discharge, e.g. related to the inception of the current pulse. This reference time is required to establish the delay of the imaging (the moment of opening of the ICCD camera) with respect to the characteristic event, and then to be able to trace the time evolution of the discharge during the exposure time of the ICCD camera. Performing a temporally resolved imaging, the procedure consists in repeated image acquisition with the incremented delay between consecutive acquisitions. Such a procedure of scanning the time delay between the event and the image is known as Boxcar scanning. Using the Boxcar

scanning, the time evolution of the discharge can be revealed.

The inception of the corona current pulse is commonly accepted as the most convenient characteristic event in both DC and pulsed coronas. However, as mentioned above, the inception of the DC corona current pulse is an uncontrolled stochastic process (due to the inception time-lag jittering), while the inception of the pulsed corona is more or less controlled by the pulsed power supply. This makes the synchronization of Boxcar scanning easier in the case of the pulsed coronas.

In the pulsed coronas, a comprehensive spatial and temporal visualization of the corona current pulse using modern high sensitive and nanosecond-fast CCD cameras was carried out by the group of Eindhoven University of Technology. The reader is referred to the publications (*7, 17, 20, 26-29*).

Below the recent progress in the visualization of the DC corona current pulses is presented.

Recent Progress in the Visualisation of the DC Positive Corona Discharges

Laser Triggering of the DC Positive Corona Streamer

To control the inception time of the DC positive corona current pulse, a technique for the controlled inception of a DC corona pulse by an UV laser beam was developed (*30-32*). As mentioned, the DC positive corona discharge is a train of more of less regular self-repetitive current pulses occurring between the electrode gap. However, when an UV laser beam pulse (of a pulse duration of about 20 ns) is shot between the electrode gap (Figure 1), an additional corona current pulse is induced (Figure 2). The laser induced corona pulse starts about 30-300 ns after the laser pulse, depending on the position of the laser beam in the gap, and it lasts over about 350 ns. At an appropriate position of the laser beam in the discharge gap the inception probability of the induced streamer is one and the inception time has a small jittering (*33, 34*). Due to it, the image of the corona pulse can be recorded with high temporal resolution using an ICCD camera with an appropriate adjusted recording delay (gate start) and exposure time. The recording delay adjustment is related to the UV laser beam pulse which plays a role of the characteristic event. Using the Boxcar scanning procedure, the time evolution of the discharge pulse can be revealed.

In the Boxcar scanning, it is important to deal with the repetitive corona current pulses of the same spatial and temporal characteristics. It was found out that the laser induced DC corona current pulses met this requirement with very high statistical probability (*33, 34*).

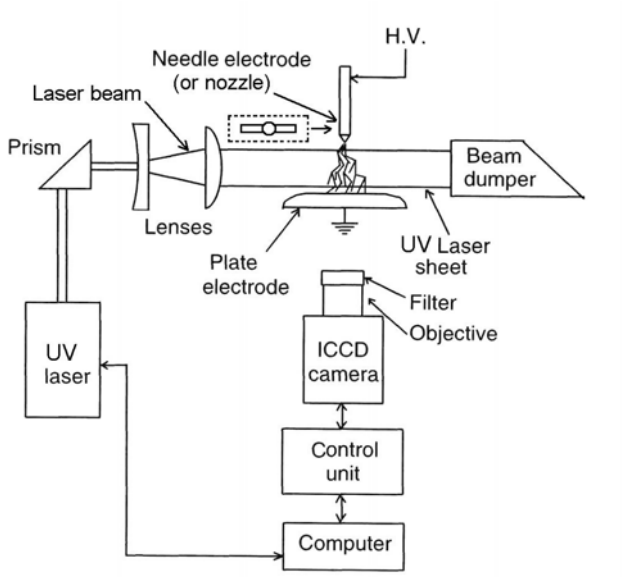

Figure 1. Setup with an ICCD camera for observation of the laser-induced DC positive corona streamers.

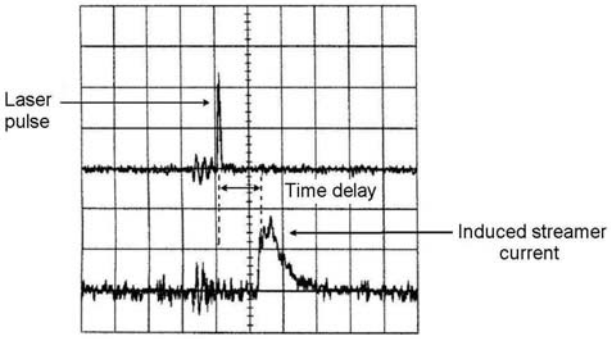

Figure 2. Time relationship between the laser beam shot and the induced DC positive corona streamer in a needle-to-plate discharge gap in air. Laser beam wavelength λ = 226 nm, laser beam pulse energy 13 mJ, gap 30 mm, DC positive voltage 25 kV, time scale 200 ns/div., current scale 20 mA/div., (*28*).

In contrast with positive coronas, no laser-induced streamer discharge was obtained for negative coronas (*33, 34*), probably due to difference in the behaviour of electrons in both discharges.

DC Corona Streamer Propagation in a Needle-to-Plate Electrode Gap

Figure 3 shows images of the streamers induced by a UV laser beam pulse of an energy of about 13 mJ in a needle-to-plate electrode gap (30 mm) in air. The DC positive voltage applied to the needle electrode was 25 kV. Each subsequent photo shows an image of the streamer recorded with an exposure time longer than the previous. In each case the ICCD camera was opened when the streamer started.

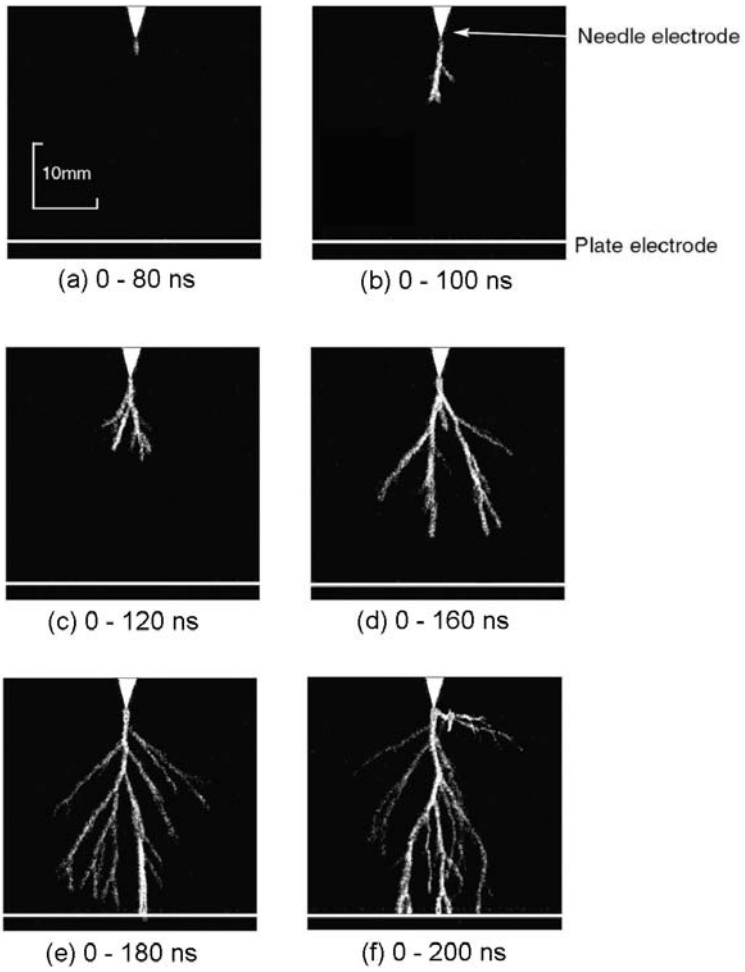

Figure 3. Time evolution of a DC positive corona streamer in a needle-to-plate electrode gap in air [(*27, 28*), see also (*25, 26, 29*)]. Laser beam wavelength λ = 226 nm, laser beam pulse energy 13 mJ, gap 30 mm, DC positive voltage 25 kV. Each image is a result of a single shot.

Because of the good reproducibility of the laser-induced streamers, the images shown in Figure 3 show time evolution of the positive corona streamer and its branching and propagation in the gas.

The images showing the time evolution of the DC positive streamer in Figure 3 may mislead the reader, who may get an impression that at a given time (e.g., at 180 ns after the streamer inception) the streamer looks as the Figure 3e shows. First of all, the ICCD camera records the relatively intense light emitted by the streamer head, the high-energy front part of the streamer. On the other hand, usually is not able the ICCD camera record the faint light emitted by the streamer channel that forms behind the streamer head. This means that the ICCD camera records the movements of the streamer head only, or in other words, the ICCD camera records the image of the streamer head pathway, which it "sees" over its exposure time. Therefore, the Figure 3e is a record of the streamer head evolution from its inception to the moment when it reaches the plate electrode, bridging the gap, i.e. during 180 ns. We may call the images presented in Figure 3 as "the time evolution of the streamer head integrated over the ICCD camera exposure time".

Fast ICCD cameras, however, give a possibility to record the image of the streamer head at a given time with a temporal resolution of about one nanosecond. Figure 4 shows different stages of the DC positive corona development on his movement from the needle electrode to plate electrode in several consecutive time intervals. Because the light emitted by an individual streamer is very faint, each image is a result of accumulation of 30 images of the individual streamers, observed with the ICCD camera with fixed both the exposure time (20 ns) and delay between the streamer inception and the opening of the ICCD camera gate. Each next image in Figure 4 was taken for the subsequent time interval. Since the laser-induced streamers are alike in appearance, the

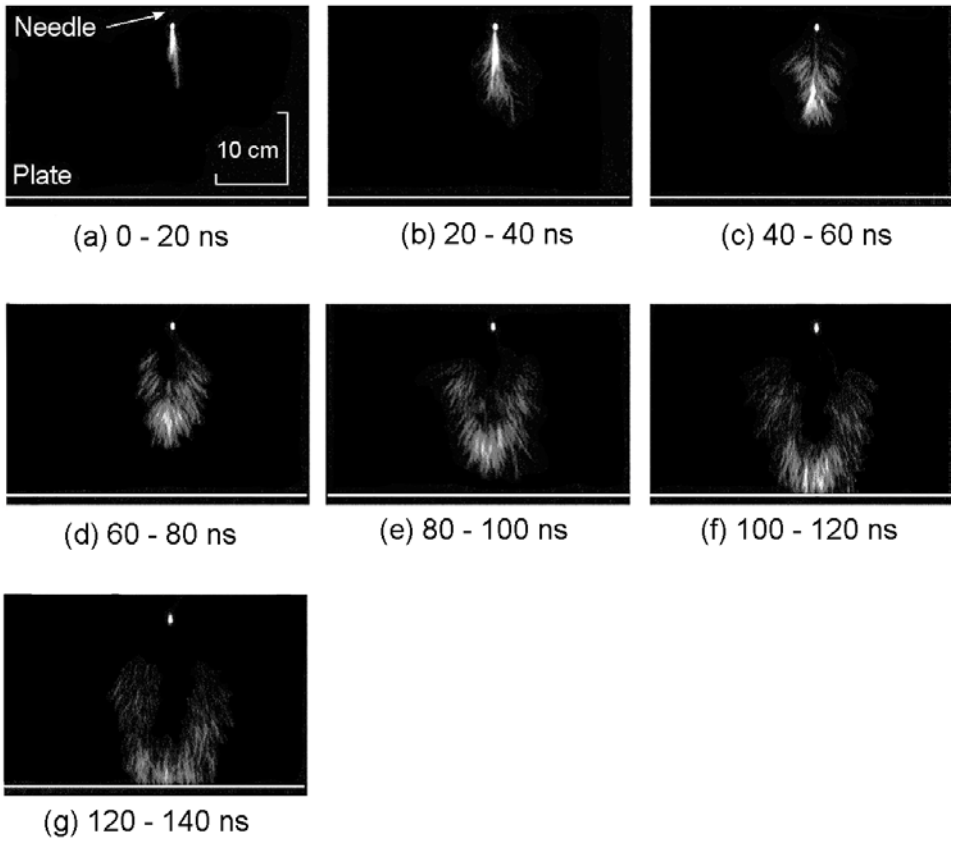

Figure 4. DC positive corona streamer head development in consecutive time intervals (of 20 ns duration) in a needle-to-plate electrode gap in air (*26, 29*). Laser beam wavelength λ = 226 nm, laser beam pulse energy 23 mJ, gap 30 mm, DC positive voltage 23 kV. Each image is an accumulation of 30 individual images.

accumulation of 30 their images reflects the actual steamer appearance.

It is seen from Figure 4 that the DC positive corona takes the form of a number of streamer heads, moving simultaneously through the gas. The number of heads increases during the propagation, which corresponds to the branching shown in Figure 3. Since the exposure time was 20 ns, each image shows the pathway the streamer head passed during 20 ns. The shape of the streamer head could not be resolved in this experiment; for that a much shorter exposure time is needed.

The time evolution of the DC positive corona streamers shown in Figures 3 and 4 makes the determination of the propagation velocity of the streamer head averaged over the exposure time (or corresponding streamer head pathway) possible. From Figure 3 it can be found that the velocity of the streamer head propagation, averaged over the gap distance, is about (2.5-3) $\times 10^5$ m/s. This is in a good agreement with the value measured with a photomultiplier in (*18*). Using a shorter exposure time interval it is possible to scan the velocity of the streamer along its trip from the needle to plate electrode (also in the lateral direction).

Figure 4 reveals an interesting feature of the DC positive corona streamer. The streamer heads emit light, whereby they are seen, or at least recorded by ICCD cameras. On the contrary, the streamer channels behind the streamer heads are dark, and thus invisible. However, a glow around the needle tip is seen over the life-time of the corona streamer, i.e. from its inception to the moment it bridges the gap. The nature of this glow is not clear.

The ICCD images make determination of the averaged streamer diameter possible. The average diameter of the streamers shown in Figure 3 is about 150 μm. This is in agreement with other measurements (*17, 27*).

DC Corona Streamer Propagation in a Nozzle-to-Plate Electrode Gap

Recently, a corona radical shower discharge has been proved to be one of the most efficient non-thermal plasmas for NO_x removal. Such a discharge is suitable for the retrofit of the existing electrostatic

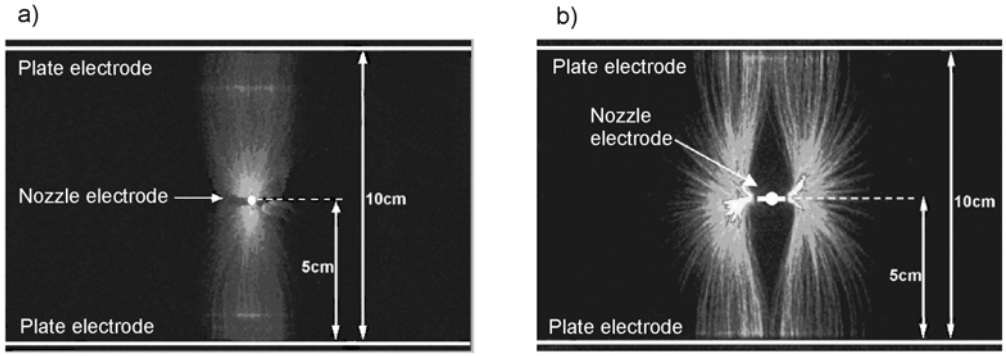

Figure 5. Images of DC positive corona streamers in a nozzle-to-plate electrode gap in NO(200 ppm)/air mixture taken with a long exposure time (0.6 ms): (a) front view and (b) side view. Gap 50 mm, DC positive voltage 27 kV, time-averaged current 0.1 mA. Each image is an average of 100 images (*34*).

precipitators (*9*). In the corona radical shower discharge reactor, the discharge electrode with one or several nozzles is used for injection of an additional gas across the corona discharge zone into the flue gas (*36-38*). The other electrodes (grounded) are plates. Therefore, the shape of the discharge in such a nozzle-to-plate electrode geometry is much complex than that of the conventional electrode arrangement, such as needle-to plate or wire-to-plate. The control of parameters of the streamer corona discharge is in the nozzle-to-plate electrode arrangement a key issue to obtain plasma suitable for NOx removal from the flue gas. Visualization of the corona discharges with an ICCD camera is an important tool for studying the parameters of the streamer corona in that electrode arrangement.

Figure 5 shows images (front and side view) of the DC positive corona streamers in a nozzle-to-plate electrode gap (50 mm) in NO(200 ppm)/air mixture taken with the ICCD camera with a long exposure time (0.6 ms). As seen, the streamers consist of several branches, propagating from the tip of the nozzle electrode to the plate electrodes. The plasma formed by the streamers looks like a flame when observed with the naked-eye or when photographed with a long exposure time, as in Figure 5.

Figure 6 shows images (side view) of the DC positive corona streamers in the nozzle-to-plate electrode gap in NO(100 ppm)/air mixture taken with the ICCD camera with a long exposure time (0.6 ms) for various operating voltages. As it is seen, the area occupied by the streamers increases with increasing voltage (and corresponding increase of the discharge current). At low voltages (< 22 kV) relatively short streamers of similar length are formed around the nozzles. With increasing voltage the length of the streamers developed in the direction of the plate electrodes becomes longer than those directed parallel to the plates. The plate-directed streamers bridge the gap at voltages higher than 24 kV. A well developed streamer corona occurs at voltages higher than 30 kV.

Figure 7 shows the time evolution of the DC positive streamer corona in the nozzle-to-plate electrode gap (50 mm) in NO(100 ppm)/air mixture. The positive voltage applied to the nozzle electrode was 30 kV, which was sufficient to get the bridged corona streamer (see Figures 7e and 7f). In each subsequent image the exposure time of the ICCD camera is longer than in the previous. The ICCD camera was opened when the streamer started. The images in Figure 3 clearly show the evolution, branching and propagation of the positive corona streamer in the gap, "integrated over the ICCD camera exposure time".

Figure 8 shows different stages of the DC positive corona streamer head development on its movement from the nozzle to the plate electrode in NO(100 ppm)/air mixture in several consecutive time intervals (duration 50 ns). The operating voltage was 30 kV. Because the light emitted by the streamer head is very faint, each image is a result of accumulation of 100 images of the individual streamers, observed with the ICCD camera with an exposure time fixed at 50 ns. Since the laser-induced streamers are alike in appearance, the accumulation of 100 their images reflects the actual steamer appearance.

As in the needle-to-plate electrode geometry, the DC positive corona shown in Figure 8 takes the form of a number of streamer heads, moving simultaneously through the gas. The number of heads increases during the propagation, which corresponds to the branching shown in Figures 6 and 7. Since the exposure time was 50 ns, each image shows the pathways the streamer heads passed during 50 ns.

It can be found from Figure 8 that the streamers directed towards the plate electrode (so-called verti-

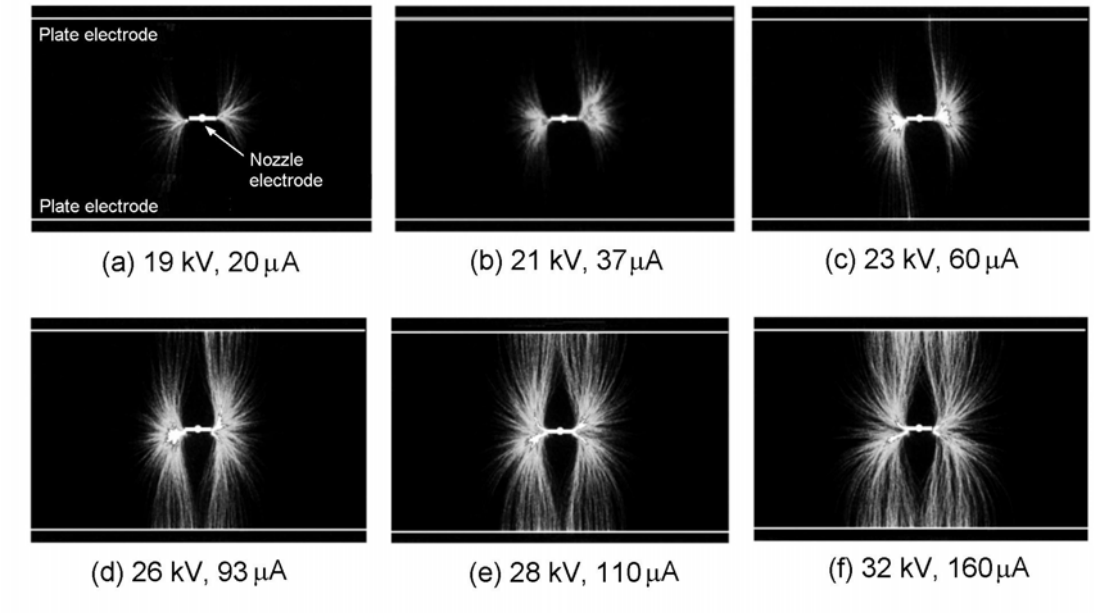

Figure 6. Images (side view) of DC positive corona streamers in a nozzle-to-plate electrode gap (50 mm) in NO(100 ppm)/air mixture taken with a long exposure time (0.6 ms) for various operating voltages. Each image is an average of 100 images.

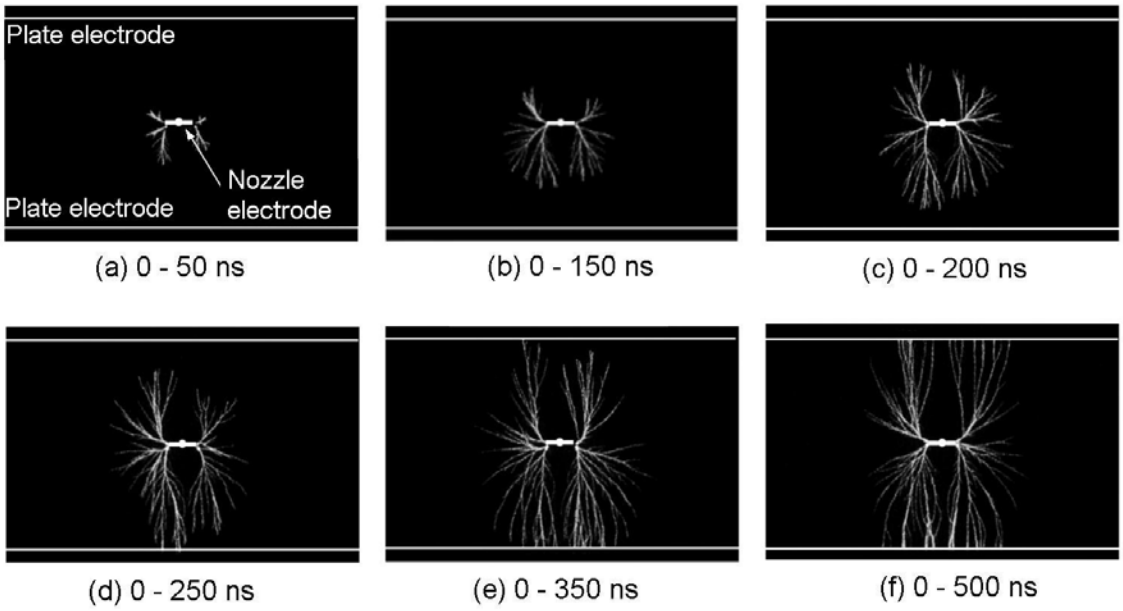

Figure 7. Time evolution of DC positive corona streamer in a nozzle-to-plate electrode gap in NO(100 ppm)/air mixture (*35*). Laser beam wavelength λ = 226 nm, laser beam pulse energy 13 mJ, gap 50 mm, DC positive voltage 30 kV, time-averaged current 134 μA. Each image is a result of a single shot (*35*).

cal streamers) are faster than those moving parallel to the plates (lateral streamers). Besides, the velocity of both of the streamers is not constant along their pathways. At 30 kV, the velocity of the vertical streamers changes from about 3.5×10^5 m/s at the nozzle (the first 50 ns) to about $(1.3\text{-}1.5)\times10^5$ m/s in the middle of the gap (time period of 50-150 ns) and at the plate electrode (200-250 ns). The vertical streamer velocity averaged over the distance from the nozzle to the plate electrode is 2.5×10^5 m/s, as that found for the streamer in the needle-to-plate gap. The velocity of the lateral streamers changes from about 1.7×10^5 m/s in the first 50 ns (at the nozzle), through about 1.3×10^5 m/s in the time period of 50-200 ns, to $(0.4\text{-}0.5)\times10^5$ m/s at 200-300 ns, i.e. when the corona extinguishes after bridging the gap.

Also Figures 7 and 8 show the presence of the glows around the nozzle tip over the life-time of the

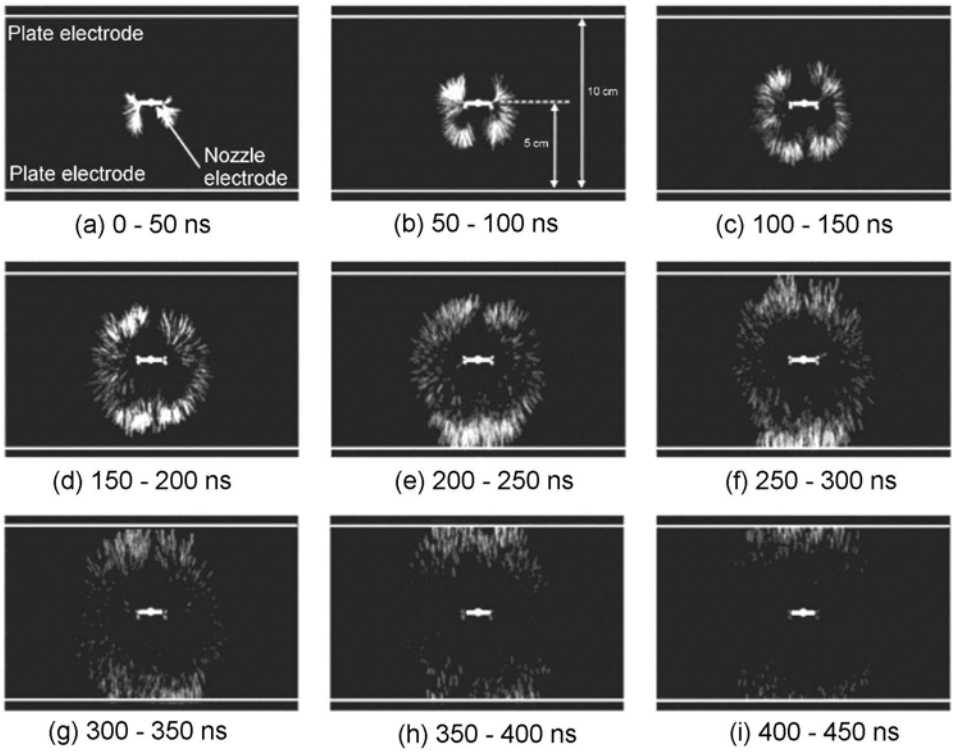

Figure 8. DC positive corona streamer head development in consecutive time intervals (of 50 ns duration) in a nozzle-to-plate electrode gap in NO(100 ppm)/air mixture. Laser beam wavelength λ = 226 nm, laser beam pulse energy 13 mJ, gap 50 mm, DC positive voltage 30 kV, time-averaged current 134 μA. Each image is an average of 100 images taken with the ICCD camera.

corona streamer, i.e. from its inception to the moment it bridges the gap, similarly as in Figure 4 for the needle-to plate geometry.

The average diameter of the streamers in the nozzle-to-plate electrode geometry found from Figures 7 and 8 is about 150 μm. This is in agreement with that found for the streamers in the needle-to-plate electrode gap.

Summary and Conclusions

Recent progress in the development of ICCD cameras, imaging spectrographs and fast digital image processing has made visualization of complex gas discharges, like DBDs and corona discharges, possible with higher sensitivity and space and time resolution than ever.

In order to perform a temporally resolved imaging of the corona discharge, the corona inception time has been assigned as a reference time to establish the delay of the imaging to be able to trace the time evolution of the discharge over the opening time of the ICCD gate. To control the inception time of the DC positive corona current pulse, a technique for the controlled inception of a DC positive corona current pulse by an UV laser beam was developed. When an UV laser beam pulse (of a pulse duration of about 20 ns) is shot between the electrode gap, an additional corona pulse is induced with an inception probability of one. The inception time of the laser induced streamer has a small jittering. Due to it, the image of the corona pulse can be recorded with high temporal resolution using an ICCD camera with an appropriate adjusted recording delay and exposure time.

Using this visualization technique, the DC positive corona streamer propagation in the needle-to-plate and nozzle-to-plate electrode gaps in air or NO/air mixtures was investigated with high resolution in space and time. The obtained images showed the time evolution of the DC positive streamer and different stages of the streamer development on its pathway from the needle or nozzle electrode to the plate electrode in several consecutive time intervals. The time evolution of the DC positive streamers made the determination of the propagation velocity of the streamer head averaged over the exposure time (or corresponding streamer head pathway) possible. The average velocity of the streamer head propagation is about (2.5-3) x 10^5 m/s.This is in agreement with other measurements.

In the case of the nozzle-to-plate geometry it was found that the streamers directed towards the plate

electrode (vertical streamers) are faster than those moving parallel to the plates (lateral streamers). In both cases the velocity of the streamers is not constant along their pathways.

The ICCD images revealed an interesting feature of the DC positive streamer corona, i.e. a glow around the needle (or nozzle) tip during the life-time of the corona streamer, i.e. from its inception to the moment it bridges the gap. The nature of this glow is not clear.

The ICCD images made determination of the averaged streamer diameter possible. The average diameter of the streamer is about 150 μm. This is in agreement with other measurements.

The presented results showed that the visualization with ICCD cameras of higher sensitivity and space and time resolution than ever offers unprecedented way of displaying the transient discharges. In particular, using sensitive ICCD cameras with a super fast optical shutter (the gate below 1 ns) would make the investigation of these discharges possible in detail. For example, the experimental study of the shape of the streamer head is of high interest. However, for that purpose a three-dimensional measurements are needed. The three-dimensional measurements are also required for a better understanding of the streamer propagation and branching.

Acknowledgments

This research was carried out under the joint Japanese-Polish project sponsored by the Japan Society for the Promotion of Science and the Polish Academy of Sciences. The authors are indebted to Prof. Jen-Shih Chang of McMaster University, Hamilton, Ontario, Canada for fruitful discussions and stimulation to write this paper.

References

(*1*) Chang, J.S.; Lawless, P.A.; Yamamoto T. *IEEE Trans. Plasma Sci*. **1991**, *19*, 1152-1165.

(*2*) Non-thermal Plasma Techniques for Pollution Control, Eds.: Penetrante, B.M.; Schultheis, S.E., NATO ASI Series G, vol. 34 A and B, Springer, Berlin, 1993.

(*3*) Vercammen, K.L.L.; Berezin, A.A.; Lox, F.; Chang, J.S. J. *Adv. Oxid. Technol*. **1997**, *2*, 312-329.

(*4*) Manheimer W., Sugiyama L.E., Stix Th.H., Eds., *Plasma Science and the Environment*, AIP Press, 1997.

(*5*) Hammer, T. *Contrib. Plasma Phys*. **1999**, *39*, 441-462.

(*6*) Urashima, K. ; Chang J.S. *IEEE Trans. Dielectrics and Electrical Insulation* **2000**, *7*, 602-614.

(*7*) Van Veldhuizen, E.M., Ed.; *Electrical Discharges for Environmental Purposes: Fundamentals and Applications*, Nova Science Publishers, Inc.: 2000; ISBN 1-56072-743-8.

(*8*) Chang, J.S. *Science and Technology of Advanced Materials* **2001**, *2*, 571-576.

(*9*) Chang, J.S. *J. Electrostatics* **2003**, *57*, 273-291.

(*10*) Loeb, L.B. *Electrical Coronas*, Univ. of California Press, 1965.

(*11*) Nasser, E. *Fundamentals of Gaseous Ionization and Plasma Electronics*, Wiley-Interscience: 1971.

(*12*) Meek, J.M. *Electrical Breakdown of Gases*, Wiley Interscience: 1978.

(*13*) Raizer, Y.P. *Gas Discharges Physics* Springer: Berlin, 1991.

(*14*) Bazelian, E.M. Raizer, Yu.P. *Spark Discharge*, MFTI, Moscow, 1997 (in Russian).

(*15*) Dyakonov, M.I.; Kachorovskii, V.Yu. *Sov. Phys. JETP* **1988**, *94*, 321-332 (in Russian).

(*16*) Kulikovsky, A.A. *J. Phys. D: Appl. Phys*. **1995**, *28*, 2483-2493.

(*17*) Van Veldhuizen, E.M.; Rutgers, W.R. *J. Phys. D: Appl. Phys.* **2002**, *35*, 2169–2179.

(*18*) Yan, K.; Yamamoto, S.; Kanazawa, S.; Ohkubo, T.; Nomoto, Y.; Chang, J.S. *J. Electrostatics* **1999**, *46*, 207-219.

(*19*) Spyrou, N.; Peyrous, R.; Gibert, A. *J. Phys. D: Appl. Phys*. **1989**, *22*, 120-128.

(*20*) Creyghton, Y.L.M. *Pulsed Positive Corona Discharges: Fundamental Study and Application to Flue Gas Treatment*, PhD Thesis, Eindhoven University of Technology, 1994.

(*21*) Allen, N.L.; Ghaffar, A. *J.Phys.D: Appl. Phys*. **1995**, *28*, 338-343.

(*22*) Reather, H. *Zeitschrift für Physik*, **1939**, *112*, 464. (Reproduced in: Electric Breakdown in Gases, Rees J.A., The Macmillan Press: London, 1973; pp 18-26).

(*23*) Wagner, K.H. *Zetschrift für Physik* **1966**, *189*, 465.

(*24*) Wagner, K.H. *Zetschrift für Physik* **1967**, *204*, 177.

(*25*) Kondo, K.; Ikuta, N. *J. Phys. D: Appl. Phys*. **1980**, *13*, L33-L38.

(*26*) Blom, P.P.M. *High-power Pulsed Corona*, PhD Thesis, Eindhoven University of Technology, ISBN 90-386-0250-2, 1997.

(*27*) Van Veldhuizen, E.M.; Baede, A.H.F.M.; Hayashi, D.; Rutgers, W.R. In *Proceedings of APP Spring Meeting*, Bad Honnef, Germany, 2001, pp 231–4.

(*28*) Valette, N. *Internal Report EPG*, Eindhoven University of Technology, 2001.

(*29*) Van Veldhuizen, E.M.; Kemps, P.C.M.; Rutgers W.R. *IEEE Plasma Sci*. **2002**, *30*, 162-163.

(*30*) Mizeraczyk, J.; Ohkubo, T.; Kanazawa, S.; Nomoto, Y. In *Proceedings of 1999 Annual Meeting of the Institute of Electrostatics Japan*, Tsudanuma, Japan, 1999; pp 231-234.

(*31*) Mizeraczyk, J.; Ohkubo, T.; Kanazawa, S.; Nomoto, Y.; Kawasaki, T.; Kocik, M. In *Laser Technology VI: Applications*, Woliński, W.L.; Jankiewicz, Z. Eds., In *Proc. of SPIE*, Vol. 4238, pp 242-245.

(*32*) Ohkubo, T.; Akamine, S.; Kanazawa, S.; Nomoto, Y.; Mizeraczyk, J. In *Proceedings of the First Polish-Japanese Hakone Group Symposium on Non-thermal Plasma Processing of Water and Air, Sopot*, Mizeraczyk, J; Dors, M. Eds., 2000, pp 85-88.

(*33*) Kanazawa, S.; Shuto, Y.; Ito, T.; Ohkubo, T.; Nomoto, Y.; Mizeraczyk, J. In *Proceedings of the Second Asia-Pacific International Symp. on the Basis and Applications of Plasma Technology, Kaohshiung*, Taiwan, 2001; pp 195-200; also In *Papers of Technical Meeting on Plasma and Pulse Power*, IEE Japan, 2001; pp 75-80.

(*34*) Kanazawa, S.; Ito, T.; Shuto, Y.; Ohkubo, T.; Nomoto, Y.; Mizeraczyk, J. *J. Electrostatics* **2002**, *55*, 343-350.

(*35*) Ohkubo, T.; Ito, T.; Shuto, Y.; Akamine, S.; Kanazawa, S.; Nomoto, Y.; Mizeraczyk, J. *J. Adv. Oxid. Technol*. **2002**, *5*(2), 129-134.

(*36*) Ohkubo, T.; Kanazawa, S.; Nomoto, Y.; Chang, J. S.; Adachi, T. *IEEE Trans. Ind. Appl*. **1994**, *30*, 856-861.

(*37*) Ohkubo, T.; Kanazawa, S.; Nomoto, Y.; Chang, J. S.; Adachi T. *IEEE Trans. Ind. Appl*. **1996**, *32*, 1058-1062.

(*38*) Kanazawa, S.; Chang, J. S.; Round, G. F.; Sheng, G.; Ohkubo, T.; Nomoto, Y.; Adachi, T. *J. Electrostatics* **1997**, *40 and 41*, 651-656.

(*39*) Kanazawa, S.; Sumi, T.; Sato, N.; Ohkubo, T.; Nomoto, Y.; Kocik, M.; Mizeraczyk, J.; Chang, J.S. *IEEE Trans. Ind. Appl*. 2003 (submitted).

(*40*) Kanazawa, S.; Sumi, T.; Simamoto, S.; Ohkubo, T.; Nomoto, Y.; Kocik, M.; Mizeraczyk, J.; Chang, J.S. *IEEE Trans. Plasma Sci*. 2003 (submitted).

Received for review October 15, 2003. Revised manuscript received November 24, 2003. Accepted December 10, 2003.